Supplementary material

Porous honeycomb-like $NiSe_2$/red phosphorus heteroarchitectures for photocatalytic hydrogen production

Jia Jia[a], Xue Bai[a,b], Qiqi Zhang[a], Xiaoyun Hu[c], Enzhou Liu[a,*], Jun Fan[a,*]

[a]School of Chemical Engineering, Northwest University, Xi'an 710069, P. R. China.

[b]College of Chemistry and Material, Northwest University, Xi'an 710069, P. R. China.

[c]School of Physics, Northwest University, Xi'an 710069, P. R. China.

*Corresponding author. Tel.: +86 29 88303679; fax: +86 29 88302223.

E-mail address: fanjun@nwu.edu.cn; liuenzhou@nwu.edu.cn

Preparation of NiS/RP Composite

The detailed synthetic process of NiS/RP composite was as follow: First, 19.26 mg of $Ni(acac)_2$ (Nickel(II) acetylacetonate, Macklin) and 0.2 g of nano RP were added into 50 mL three-neck flask containing a mixed solution of OLA (10 mL, oleylamine), OA (0.25 mL, oleic acid) and ODE (15 mL, 1-octadecene), and to acquire an uniform suspension solution with the aid of continuous stirring and nitrogen flowing atmosphere (Solution A). After stirring for 30 min, the above solution was quickly preheated up to 175 ^{o}C. Subsequently, 800 μL of DT (1-dodecanethiol) solution was rapidly added into Solution A and held for 30 min to obtain a lot of black product, suggesting the synthesis of NiS/RP composite. Finally, the formed precipitate was centrifuged and washed with several times using the chloroform and ethanol solution in order to dislodge residual solvent, and then dried at 45 ^{o}C for 6 h under nitrogen flowing atmosphere. At the same time, this sample was marked as 8.1% NiS/RP. For comparison, the y_2%-NiS/RP (y_2= 2.7, 5.4, and 10.7) were prepared via a similar synthetic method (y_2 represents theoretical adding amount of NiS).

Preparation of NiS/RP Composite

The detailed synthetic process of FeS/RP composite was as follow: First, 16.60 mg of $Fe(acac)_3$ (Iron(III) acetylacetonate, Macklin) and 0.2 g of nano RP were added into 50 mL three-neck flask containing a mixed solution of OLA (10 mL, oleylamine), OA (0.25 mL, oleic acid) and ODE (15 mL, 1-octadecene), and to acquire an uniform suspension solution with the aid of continuous stirring and nitrogen flowing atmosphere (Solution A). After stirring for 30 min, the above solution was quickly preheated up to 175 ^{o}C. Subsequently, 800 μL of DT (1-dodecanethiol) solution was rapidly added into Solution A and held for 30 min to obtain a lot of black product, suggesting the synthesis of FeS/RP composite. Finally, the formed precipitate was centrifuged and washed with several times using the chloroform and ethanol solution in order to dislodge residual solvent, and then dried at 45 ^{o}C for 6 h under nitrogen flowing atmosphere. At the same time, this sample was marked as 5.3% NiS/RP. For comparison, the y_3%-FeS/RP (y_2= 2.6, 8.0, and 10.6) were prepared via a similar synthetic method (y_3 represents theoretical adding amount of FeS).

Photoelectrochemical characterization

A series of photoelectrochemical measurements, for example Mott-Schottky plots (from -0.6 V to 1.0 V vs. SCE), electrochemical impedance spectra (at 0.5 V bias potential vs. SCE, frequency range from 0.01 to 10^5 Hz), linear sweep voltammetry (from 0.0 V to 0.7 V vs. SCE), transient photocurrent

(at 0.5 V bias potential vs. SCE) and HER polarization curves (from -1.0 V to 0.0 V vs. SCE), were analyzed on the CHI660E electrochemical workstation under 300 W Xe lamp, of which the counter electrode, reference electrode and working electrode were Pt, saturated calomel electrode (SCE) and photoanode. The irradiation area and electrolyte solution were 0.785 cm^2 and 0.5 M Na_2SO_4 solution (pH = 7.0), respectively. In addition, the photoanode was synthesized according to the following methods: 5 mg of catalyst was dispersed into a mixed solution of ethanol/water (1 mL and the volume ratio is 1:1) and treated several times in ultrasound. Subsequently, the above suspension solution was directly dripped onto the FTO conductive glass surface by a disposable dropping pipette and then drying at 30 °C for all night.

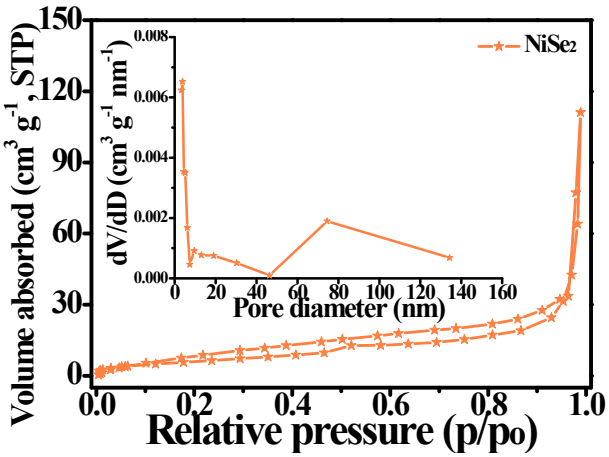

Fig. S1 N_2 adsorption-desorption isotherms and pore size distribution plots of pristine $NiSe_2$.

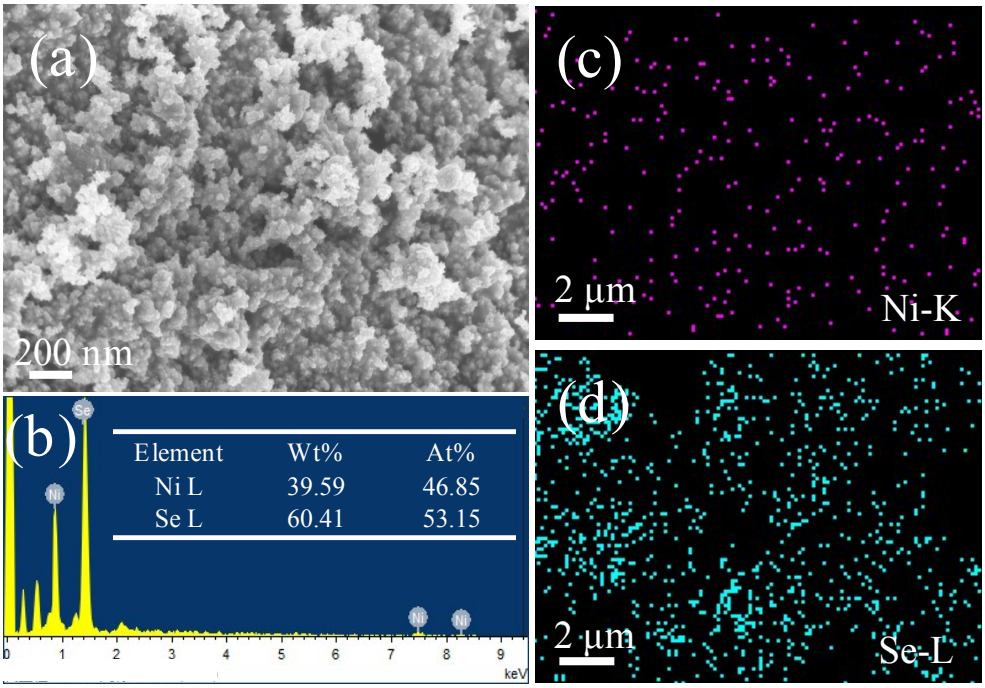

Fig. S2 The (a) SEM, (b) EDS and (c, d) EDS Mapping of as-prepared $NiSe_2$ samples.

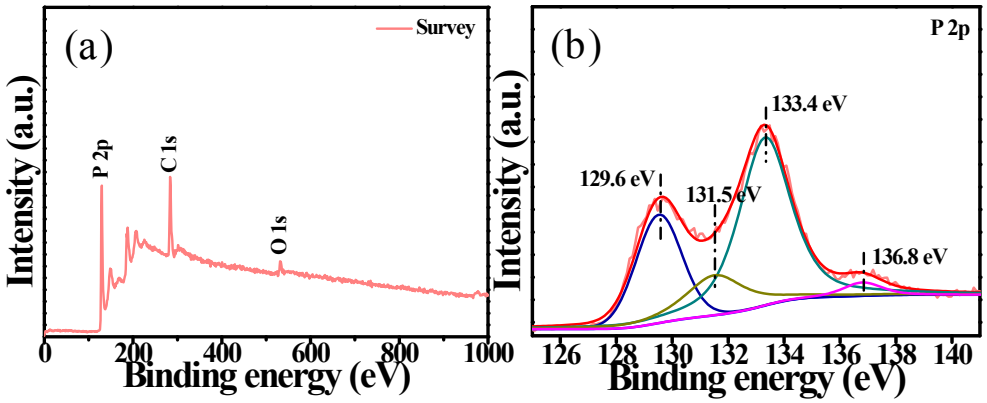

Fig. S3 (a) XPS survey and (b) high resolution XPS spectrum of P 2p for pure RP.

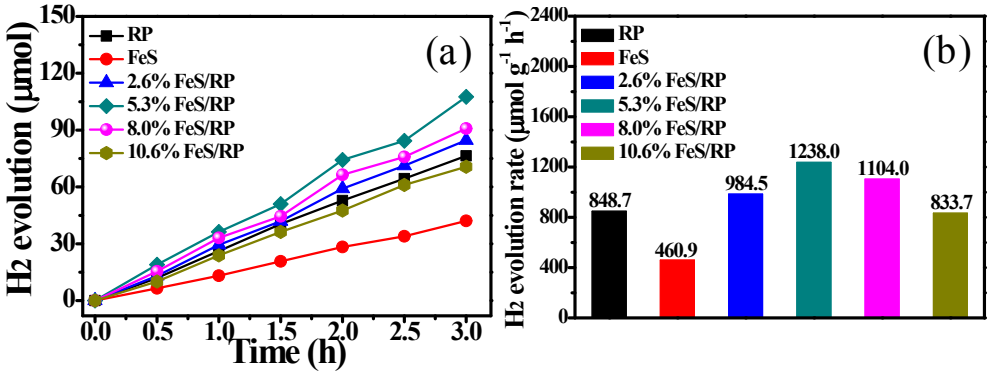

Fig. S4 (a) Photocatalytic H_2 generation amounts and (b) H_2 generation rates for different FeS/RP under light irradiation.

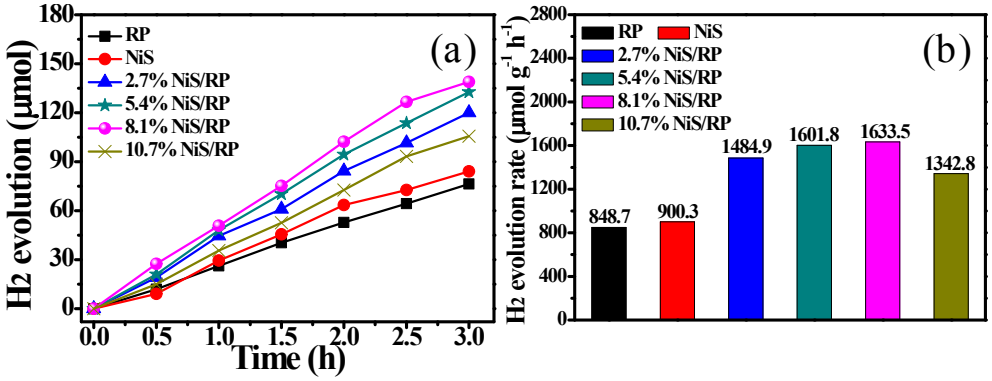

Fig. S5 (a) Photocatalytic H_2 generation amounts and (b) H_2 generation rates for different NiS/RP under light irradiation.

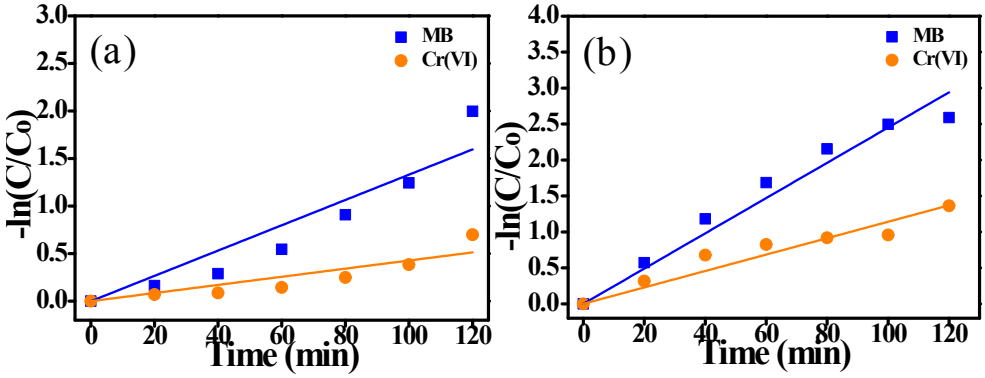

Fig. S6 The removal rate constant (K_{app}) of Cr(VI) and MB over (a) pure RP and (b) 5.4% $NiSe_2$/RP composite.

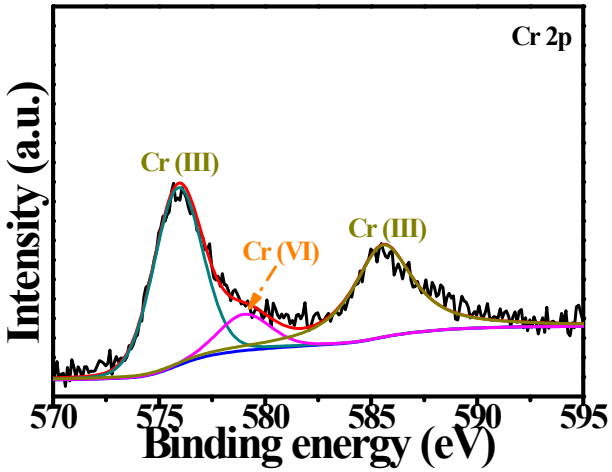

Fig. S7 High resolution XPS spectra of Cr on the surface of 5.4% $NiSe_2$/RP composite after the photocatalytic reaction.[1-3]

The electron lifetime (τ_n) of the as-prepared photoanodes can be calculated from the Bode phase plots according to the following Equation S1:[4]

$$\tau_n = \frac{1}{2\pi f_{max}} \qquad \text{(S1)}$$

Where, τ_n and f_{max} is the electron lifetime and the maximum frequency value, respectively.

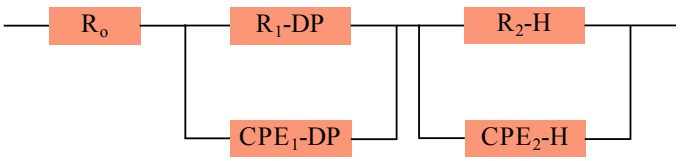

Fig. S8 The equivalent circuit model of the Nyquist plots.

As shown in Fig. S9a, the photocurrent density of $NiSe_2$ photoanode is about 9.8 uA/cm^2, which is lower than that of 5.4% $NiSe_2$/RP (16.8 uA/cm^2). Besides, Fig. S9b illustrates that pure $NiSe_2$ has a low resistance compared to RP and 5.4% $NiSe_2$/RP composite, which may be due to good conductivity of $NiSe_2$ itself.

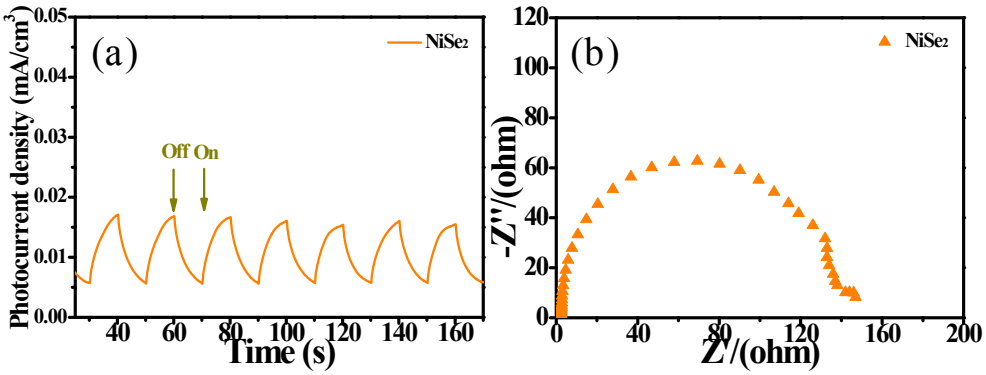

Fig. S9 (a) Transient photocurrent density and (b) EIS curves of pure $NiSe_2$.

According to the fitted results of time-resolved transient PL decay curves, the PL average decay lifetime (τ) of the obtaining sample is calculated by the following Eq. S2:[5]

$$\tau = \tau_1 A_1 + \tau_2 A_2 \qquad \text{(S2)}$$

Where, τ is the average decay lifetime, τ_1 and A_1 as well as τ_2 and A_2 are the fast and minority-slow decay component, respectively.

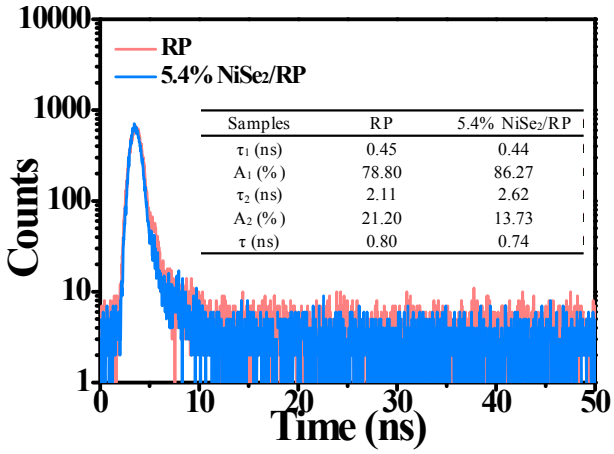

Samples	RP	5.4% $NiSe_2$/RP
τ_1 (ns)	0.45	0.44
A_1 (%)	78.80	86.27
τ_2 (ns)	2.11	2.62
A_2 (%)	21.20	13.73
τ (ns)	0.80	0.74

Fig. S10 Time-resolved PL decay spectra and calculated average lifetime of pristine RP and 5.4% $NiSe_2$/RP heterostructure.

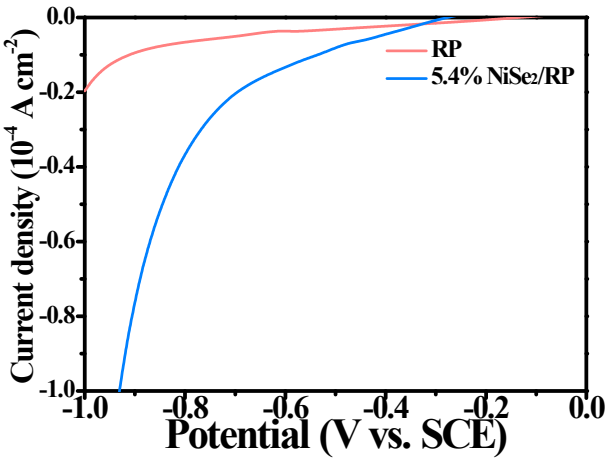

Fig. S11 The HER polarization curves of RP and $NiSe_2$/RP photoanode.

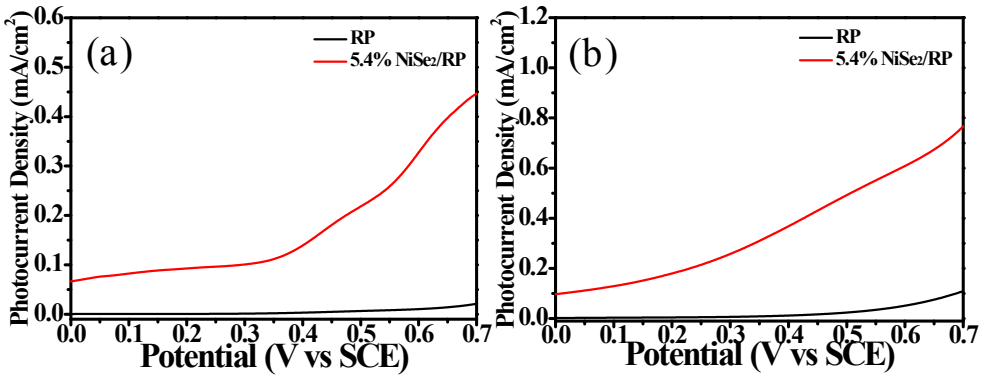

Fig. S12 Linear sweep voltammetry for RP and 5.4% $NiSe_2$/RP measured in (a) 0.5 M Na_2SO_4 as well as (b) in 0.35 M Na_2S and 0.25 M Na_2SO_3 solution under solar light irradiation.

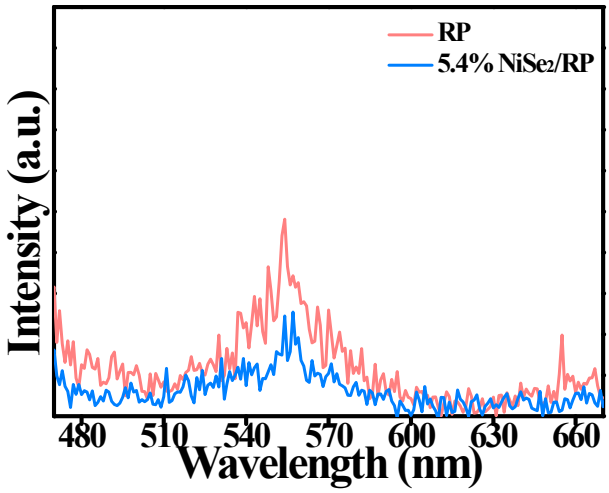

Fig. S13 PL spectra of RP and 5.4% $NiSe_2$/RP composite.

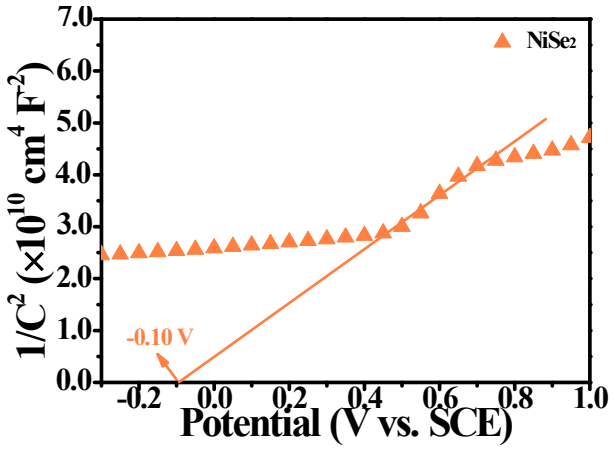

Fig. S14 Mott-Schottky plot of pure $NiSe_2$.

The electron-transfer number (n) is determined by a rotating ring-disk electrode (RRDE) electrochemical measurement including a glassy carbon disk with 5.4% $NiSe_2$/RP sample (Φ:5.61 mm, disk area: 0.247 cm^2, ring area: 0.185 cm^2), Pt ring and Ag/AgCl as reference electrode, based on the following Equation S3:6

$$n = \frac{4I_{disk}}{I_{disk} + \frac{I_{ring}}{N}} \qquad \text{(S3)}$$

Where N is the RRDE collection efficiency, measured to be 0.39, I_{ring} and I_{disk} are the ring and disk current. In general, at the ring potential of -0.3 V, the trace amount of oxygen species such $\cdot O_2^-$, H_2O_2 and ·OH will be generated. Therefore, we detect this potential to determine the formation of H_2O_2.

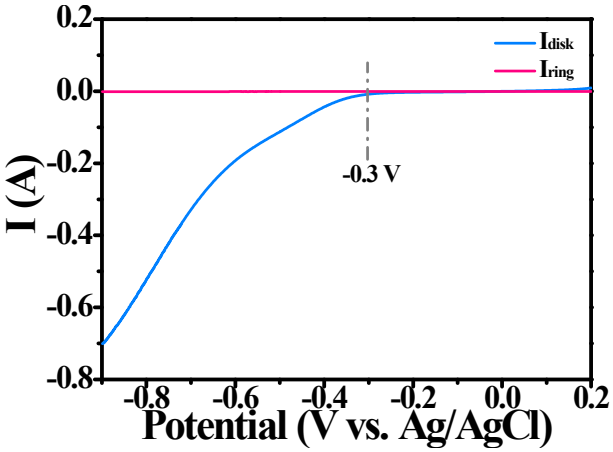

Fig. S15 The I-V curve of 5.4% $NiSe_2$/RP composite based on rotating ring-disk electrode (RRDE) electrochemical measurement.

Table S1. The BET specific surface areas of different samples.

Samples	S_{BET} (m^2/g)	Average pore size (nm)	Pore volume (cm^3/g)
RP	13.6	0.02	3.09
5.4% $NiSe_2$/RP	13.2	0.02	3.08
$NiSe_2$	22.6	3.87	0.16

Table S2. Recent reports on RP-based heterojunction photocatalysts for H_2 generation.

Photocatalyst system	Sacrificial agent	Light source	Activity/($\mu mol \cdot g^{-1} \cdot h^{-1}$)	Ref.
5.4% $NiSe_2$/RP	Na_2S/Na_2SO_3	300 W Xe lamp	1968.8	This work
8.1% NiS/RP	Na_2S/Na_2SO_3	300 W Xe lamp	1633.5	This work
5.3% FeS/RP	Na_2S/Na_2SO_3	300 W Xe lamp	1230.8	This work
Crystalline RP	Methanol with 1wt% Pt as cocatalyst	300 W Xe lamp with a 400 nm cutoff filter	19.2	7
Fibrous phase RP	Methanol with 1wt% Pt as cocatalyst	300 W Xe lamp with a 420 nm cutoff filter	633.0-684.0	8
Au/RP	TEOA	300 W Xe lamp with a 420 nm cutoff filter	189.4	9
Cu/RP	TEOA	300 W Xe lamp with a 420 nm cutoff filter	225.8	9
Ni_2P/RP	TEOA	300 W Xe lamp with a 420 nm cutoff filter	240.93	10
TiO_2/RP	Methanol	300 W Xe lamp with a 420 nm cutoff filter	276.5	11
RP/g-C_3N_4	TEOA with 1wt% Pt as cocatalyst	300 W Xe lamp with a 420 nm cutoff filter	1691.0	12
GO/RP	TEOA	150 W Xe lamp with a 420 nm cutoff filter	65.0	13
$Ni(OH)_2$/RP	Methanol with 1wt%	300 W Xe lamp with a	33.0	14

	Pt as cocatalyst	400 nm cutoff filter		
g-C_3N_4/RP/MoS_2	TEOA	300 W Xe lamp with a 420 nm cutoff filter	859.7	15

Table S3. The equivalent circuit parameters for RP and $NiSe_2$/RP photoanode.

Sample	Solution	Space charge layer			Double charge layer		
	R_s (Ω)	R_1-DP (kΩ)	CPE_1-DP (μF)	Electron lifetime (μs)	R_2-DP (Ω)	CPE_2-DP (μF)	Electron lifetime (ms)
RP	2.1	15.2	4.5	34.3	33.2	13.9	3.4
$NiSe_2$/RP	2.7	13.4	14.3	74.1	96.9	6.7	15.7

Table S4. Photocurrent density-applied potential for RP and 5.4% $NiSe_2$/RP photoanode with and without the hole sacrificial agent.

Potential	***J* (μA/cm^2, Na_2SO_4)**		***J* (μA/cm^2, Na_2S/Na_2SO_3)**	
(V vs SCE)	**RP**	**5.4% $NiSe_2$/RP**	**RP**	**5.4% $NiSe_2$/RP**
0.05	0.491	76.05	2.778	111.8
0.1	0.536	82.35	3.404	129.3
0.15	0.588	88.56	3.946	151.5
0.2	0.671	92.65	4.532	179.9
0.25	0.481	96.3	5.377	214.5
0.3	1.246	100.8	6.712	257.7
0.35	2.015	111.7	8.8	309.7
0.4	3.241	139.2	11.98	368.1
0.45	4.843	180.6	16.77	430.5
0.5	6.558	218.1	23.96	492.2
0.55	8.264	258.9	34.87	551.1
0.6	10.38	327.4	51.26	608.6
0.65	14.11	397.4	75.46	674.1
0.7	21.09	446.7	109.3	766.3

References

1 H. Fida, S. Guo and G. K. Zhang, *J. Colloid Interface Sci.*, 2015, **442**, 30-38.

2 J. Matusik and T. Bajda, *J. Colloid. Interface Sci.*, 2013, **398**, 74-81.

3 X. Meng, G. Zhang and N. Li, *Chem. Eng. J.*, 2016, **314**, 249-256.

4 H. Wang, Y. H. Liang, L. Liu, J. S. Hu, P. Wu and W. Q. Cui, *Appl. Catal. B-Environ.*, 2017, **208**, 22-34.

5 W. T. Bi, L. Zhang, Z. T. Sun, X. G. Li, T. Jin, X. J. Wu, Q. Zhang, Y. Luo, C. Z. Wu and Y. Xie, *ACS Catal.*, 2016, **6**, 4253-4257.

6 W. J. Zhang, Y. Hu, C. Z. Yan, D. C. Hong, R. P. Chen, X. L. Xue, S. Y. Yang, Y. X. Tian, Z. X. Tie and Z. Jin, *Nanoscale*, 2019, **11**, 9053-9060.

7 F. Wang, W. K. H. Ng, J. C. Yu, H. J. Zhu, C. H. Li, L. Zhang, Z. F. Liu and Q. Li, *Appl. Catal. B-Environ.*, 2012, **111**, 409-414.

8 Z. F. Hu, L. Y. Yuan, Z. F. Liu, Z. R. Shen and J. C. Yu, *Angew. Chem.*, 2016, **128**, 9732-9737.

9 L. L. Qi, K .Y. Dong, T. Zeng, J. Y. Liu, J. Fan, X. Y. Hu, W. L. Jia and E. Z. Liu, *Cataly. Today*, 2018, **314**, 42-51.

10 E. Z. Liu, L. L. Qi, J. B. Chen, J. Fan and X. Y. Hu, *Mater. Res. Bull*., 2019, **115**, 27-36.

11 J. Wang, D. K. Zhang, J. K. Deng and S. J. Chen, *J. Colloid. Interf. Sci.*, 2018, **516**, 215-223.

12 W. J. Wang, G. Y. Li, T. C. An, D. K. L. Chan, J. C. Yu and P. K. Wong, *Appl. Catal. B-Environ.*, 2018, **238**, 126-135.

13 W. B. Li, Y. P. Zhang, G. D. Tian, S. Y. Xie, Q. Q. Xu, L. Wang and J. M. Tian, *J. Mol. Catal. A-Chem.*, 2016, **423**, 356-364.

14 H. F. Dang, X. F. Dong, Y. C. Dong, H. B. Fan and Y. F. Qiu, *RSC. Adv.*, 2014, **4**, 44823-44826.

15 H. Zhao, S. N. Sun, Y. Wu, P. P. Jiang and Y. M. Dong, *Carbon*, 2017, **119**, 56-61.